

Surface-exosphere coupling due to thermal tides

Jeffrey M. Forbes,¹ Sean L. Bruinsma,² Xiaoli Zhang,¹ and Jens Oberheide³

Received 16 April 2009; revised 16 June 2009; accepted 18 June 2009; published 7 August 2009.

[1] Using densities measured by accelerometers on the CHAMP and GRACE satellites, and taking advantage of the local time precession characteristics of these near-polar orbiting satellites, exosphere temperatures are derived as a function of local time, longitude and latitude. Significant longitude variability (e.g., $\pm 25\text{K}$ maximum to minimum over the equator) in geomagnetically-quiet exosphere temperatures is shown to exist, and is attributed to a spectrum of diurnal and semidiurnal thermal tides that are excited in the troposphere and strongly influenced by the global land-sea distribution. Since exosphere temperatures are independent of height, this discovery constitutes evidence that exosphere variability is linked to surface variability. Recent evidence suggests that analogous effects exist at Mars. **Citation:** Forbes, J. M., S. L. Bruinsma, X. Zhang, and J. Oberheide (2009), Surface-exosphere coupling due to thermal tides, *Geophys. Res. Lett.*, 36, L15812, doi:10.1029/2009GL038748.

1. Introduction

[2] As solar radiation passes over the Earth's surface, the production and convection of water vapor and its subsequent condensation releases latent heat over a diurnal cycle. A spectrum of diurnal (24-h) and semidiurnal (12-h) thermal tides is generated that reflect the land-sea distribution and other factors. Some of these tides, namely those with sufficiently long vertical wavelengths to withstand dissipative processes along the way, reach the base of the thermosphere (ca. 100 km) [Hagan and Forbes, 2002, 2003].

[3] Hagan and Forbes [2002, 2003] estimated global distributions of latent heating from satellite data, and used a numerical model to predict the spectrum of thermal tides reaching the thermosphere. Forbes et al. [2006, 2008] and Zhang et al. [2006] analyzed temperature measurements from the SABER instrument on the TIMED spacecraft to provide an observational perspective of this tidal spectrum. There is general agreement that the predominant wave-4 longitude distribution of land-sea difference [e.g., Yagai, 1989] leads to a predominance of tidal components that impose a striking wave-4 longitude distribution on the lower thermosphere. This situation is not unique to Earth; through the kinematic lower boundary condition [Zurek, 1976; Conrath, 1976] the predominant wave-2 topography on Mars similarly leads to a wave-2 density structure in its lower

thermosphere [Forbes and Hagan, 2000; Forbes et al., 2002, 2006; Moudden and Forbes, 2008].

[4] Vertically-propagating tides reach their maximum amplitudes in the 100–150 km height region where molecular dissipation begins to dominate their behavior [Forbes and Garrett, 1979]. This altitude regime overlaps with the so-called dynamo region, where tidal motions are capable of generating electric fields. As summarized by Forbes et al. [2008, p. 2]: “It is here that winds move positive ions through collisions while electrons remain fixed to magnetic field lines due to their high gyrofrequency/collision frequency ratio; a current is thus induced. In order to maintain nondivergent flow of total electric current in accord with Maxwell's steady-state equations, a polarization electric field is set up almost instantaneously. This phenomenon is referred to as the ‘E-region wind dynamo’. These polarization electric fields are transmitted from the low- and middle-latitude E-region to the equatorial F-region along equipotential magnetic field lines. There, they modulate the background zonal electric field and the accompanying daytime ExB vertical drift that redistributes plasma upward and poleward to produce the so-called ‘equatorial anomaly peaks’ near $\pm 15\text{--}20^\circ$ magnetic latitude.”

[5] The above dynamo effect on the ionosphere is ‘indirect’ in that it relies upon the intermediary generation of electric fields, rather than being a direct result of the tidal motions themselves. In the present work, we provide evidence that the tidal perturbations themselves extend all the way to the exosphere, and impose longitude variability there in much the same way that has been documented for the lower thermosphere [e.g., Zhang et al., 2006]. We do this through analyses of CHAMP and GRACE accelerometer measurements, that are processed in a way to provide exosphere temperatures over a full range of local times, latitudes and longitudes. In their analysis of zonal winds inferred from CHAMP accelerometer measurements, Lühr et al. [2007] allude to the possibility that their detection of a wave-4 longitude structure may be more consistent with direct vertical propagation than in-situ excitation, and Oberheide and Forbes [2008] provide further evidence for this interpretation.

2. Data and Analysis Method

[6] The basic data to be employed in this study are thermosphere total mass densities inferred from accelerometer measurements on the CHAMP and GRACE satellites, which are in near-polar orbits and have been supplying data since July, 2000 and March, 2002, respectively. See Bruinsma et al. [2004, and references therein; 2006, and references therein] for various details relating to the derivation of densities from accelerometer measurements. In order to derive diurnal and semidiurnal tides, sampling over 24 hours of local time is required. CHAMP and GRACE each require more than 4 months to completely sample a solar day. However, due

¹Department of Aerospace Engineering Sciences, University of Colorado, Boulder, Colorado, USA.

²Department of Terrestrial and Planetary Geodesy, Centre Nationale D'Etudes Spatiales, Toulouse, France.

³Physics Department, University of Wuppertal, Wuppertal, Germany.

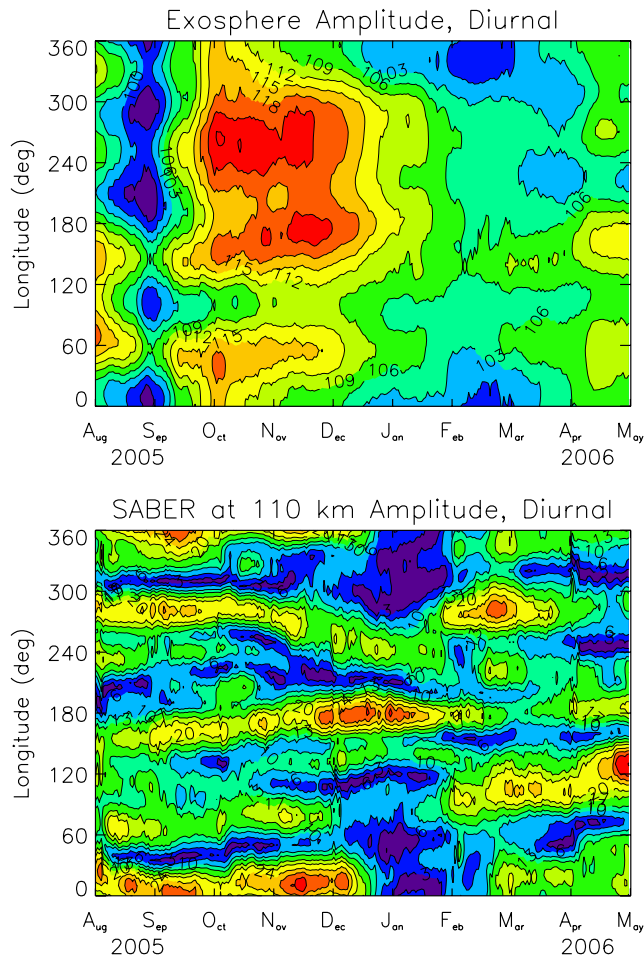


Figure 1. Equatorial tidal temperature amplitudes as a function of longitude and month from August 2005 to May 2006. (top) Exosphere temperatures, ranging from 97K (maroon) to 121K (red). (bottom) SABER temperatures at 110 km, ranging from 3K (maroon) to 27K (orange).

to the relative local time precession rates of the CHAMP and GRACE orbits, there are two periods of time wherein complete local time coverage is obtained within sequential 72-day periods: July 2005 to June 2006 (“period 1”), and December 2003 to October, 2004 (“period 2”). The problem remains that CHAMP and GRACE are acquiring data at different altitudes and both of their orbits are not exactly circular. We address this by iteratively deriving exosphere temperatures from the measured densities using the NRLMSISE-00 empirical model [Picone *et al.*, 2002]; this is possible since total density in the model depends parametrically on the temperature. The densities were first intercalibrated to remove possible biases due to drag coefficients and other effects by computing the measured/model ratios for both CHAMP and GRACE for each year; this ratio was found to be constant ($1.23 \times \text{GRACE} = \text{CHAMP}$) for both years of analysis, and yielded a ratio close to unity. And because exosphere temperatures are height-independent over the height region of interest (ca. 350–500 km), these data can be mixed together in a least-squares fitting procedure to extract the diurnal and semidiurnal tidal components.

[7] As noted by Bruinsma *et al.* [2004], uncertainty in the drag coefficient is about 5–15% and is the most important

systematic error. Errors relating to calibration, resolution, attitude, mass, and the satellite macromodel are all less than 1% for both systematic and noise errors. The largest source of error in inferring densities from in-track accelerations is due to neutral winds. In the following section, in connection with Figure 3, we show that the effects of winds are small, and validate our derived exosphere temperature structures against tidal theory. What is important for the present analysis is that the exosphere temperatures derived from CHAMP and GRACE are consistent with each other in the context of NRLMSISE-00, although they may collectively contain some bias imposed by NRLMSISE-00. Since we are primarily considering diurnal and semidiurnal variations about a background state, we maintain that any such effects will not influence the conclusions of this paper. Moreover, NRLMSISE-00 does not contain the types of tidal longitude variations that we reveal in the next section, so there is no way that our results could originate through the density-temperature conversion process.

3. Results

[8] The results presented in the following are obtained by sequentially fitting diurnal, semidiurnal and terdiurnal harmonics to 24 hours of exosphere temperature data in local time and longitude within a 72-day window, and moving this window forward one day at a time. Only measurements when $K_p < 3$ are considered. The first example is shown in Figure 1, and corresponds to the equator. The top panel illustrates the diurnal temperature amplitude as a function of longitude and time during period 1, and the bottom panel illustrates 60-day running mean diurnal temperature amplitudes at 110 km derived from the SABER instrument on the TIMED spacecraft during the same period of time, and using the same measurements that are analyzed by Forbes *et al.* [2008]. Note that the exosphere temperature transitions from a longitude wave-4 structure during August to more of a wave-3 structure during October–January, consistent with the transition from predominance of a $DE3$ to $DE2$ non-migrating tide propagating from the lower atmosphere into the upper thermosphere [Forbes *et al.*, 2008]. (As described by Forbes *et al.* [2008], DEs is short-hand notation for the eastward-propagating diurnal tide with zonal wavenumber s .) Furthermore, $DE3$ ($DE2$) gives rise to a wave-4 (–3) longitude structure for the total diurnal wave amplitude when interfering with the migrating or sun-synchronous tide $DW1$, as explained by Zhang *et al.* [2006]. For more than two waves interfering with each other, the pattern is more complicated [Angelats i Coll and Forbes, 2002].

[9] Figure 1 (top)/(bottom) imply max/min longitude variations in exosphere temperature of order $\pm 20\text{K}$ ($\pm 25\text{K}$) due to the diurnal tide alone. Note that the patterns are quite different at 110 km and in the upper thermosphere (ca. 400 km). The longitude variability of diurnal temperature amplitude evolves with altitude due to several effects. First, there is a strong diurnal exosphere temperature component that is excited in-situ in the thermosphere due to absorption of EUV radiation, and that constructively and destructively interferes differently with the non-migrating tide near 400 km than is the case at 110 km where the in-situ-driven component is much less in comparison. Further, the various vertically-propagating tides, including and in addition to $DE3$ and $DE2$,

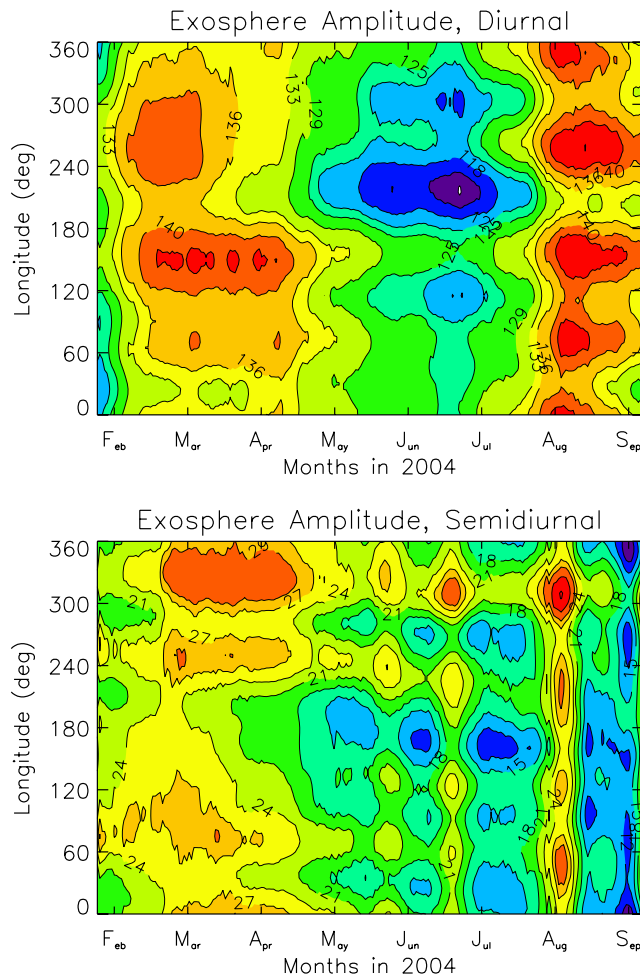


Figure 2. Equatorial tidal exosphere temperature amplitudes as a function of longitude and month from February 2004 to September 2004. (top) Diurnal amplitudes, ranging from 115K (maroon) to 144K (red). (bottom) Semidiurnal amplitudes, ranging from 9K (maroon) to 31K (red).

are affected differently by molecular dissipation, such that the relative mixture of tidal components is different between 110 km and ca. 400 km. For instance, *DE2* has a longer vertical wavelength than *DE3*, and it therefore penetrates more efficiently into the thermosphere than *DE3* (see *Forbes and Garrett* [1979] for a review of these concepts). It is also possible that these upward-propagating tidal components interact with the longitude-dependent ion drag to create other longitude-dependent structures, along the lines of the “ion drag coupling” process reviewed by *Forbes and Garrett* [1979]. It is also possible that in-situ wave-wave nonlinear interactions may induce some longitude structure [*Hagan et al.*, 2009] in the thermosphere. However, as we show below, at least for *DE3* and *DE2*, evidence points to direct vertical propagation into the thermosphere.

[10] Figure 2 provides results for period 2. The diurnal exosphere temperature structure is once again predominantly wave-4 in August, and tends to be more wave-3 in nature for the remainder of the year. This may be due to the more efficient penetration into the thermosphere by *DE2* than *DE3* as noted above. The semidiurnal tide illustrated in

Figure 2 is also predominantly wave-3 during March–April, but has periods of wave-4 predominance between May and August.

[11] In Figure 3, we perform a form of validation of our exosphere temperature results while also providing further insight. Here we utilize the methodology of “Hough Mode Extensions (HMEs)” presented by *Svoboda et al.* [2005] and utilized by *Oberheide and Forbes* [2008] to relate lower-thermosphere tidal structures with those at higher altitudes in the thermosphere. Figures 3a and 3b illustrate the latitude versus time structures of the *DE3* tidal component derived from (top) the CHAMP-GRACE data and (bottom) the SABER temperatures at 110 km. Note the similarity in latitudinal and temporal behaviors, suggesting that the exosphere temperature perturbations originate due to vertical propagation from below. Figures 3c and 3d illustrate the HME fit to (bottom) the 110 km data from SABER and (top) the exosphere temperature perturbation predicted by the upward-extended HME that was fit to the SABER temperatures. The similarity in latitude structure and amplitudes with the CHAMP-GRACE values indicates consistency of this interpretation in the context of a tidal model that takes into account molecular dissipation of a vertically-propagating tide. Figures 3e–3h illustrate the corresponding results for *DE2*. Note that *DE2* maximizes during October–February and March–April, consistent with our interpretations in Figures 1 and 2. The consistency of the HME and observed structures at 110 km is to be expected, since the HME fit is based on the illustrated data. Again, however, the predicted *DE2* exosphere temperature structure is very similar to the observations, even to the degree that significant latitudinal broadening is occurs between 110 and ca. 400 km altitude. The illustrated correspondence between these results demonstrates that the longitudinal tidal structures seen in the upper thermosphere represent the vertical propagation of non-migrating tides upwards from the base of the thermosphere.

[12] Some estimate of the effects of winds on the exosphere temperatures derived here can be obtained from the results of *Lühr et al.* [2007]. These authors demonstrate that the wave-4 longitude variability in zonal winds is of order 25 ms^{-1} , which translates to an error of 3% in density, or about 1K in exosphere temperature based on NRLMSISE-00. Similar errors are expected when *DE2* is dominant and yielding a wave-3 longitude structure. Further, it must be remembered that these waves are predominantly Kelvin waves, which have much smaller meridional winds associated with them than zonal winds. Therefore, the above error estimates due to assumption of zero winds in the derivation of in-track densities from accelerometer measurements are likely to be far in excess of the actual errors.

4. Conclusions

[13] As noted in the introduction, there is a large body of evidence that indicates that the longitudinal variability in tidal oscillations in the lower thermosphere (ca. 110 km) originates from tropospheric heating processes that reflect land-sea distributions, topography, and other factors. We demonstrate here that such influences extend to the exosphere, and we may thus conclude that exosphere variability at Earth is linked to processes occurring near the Earth’s

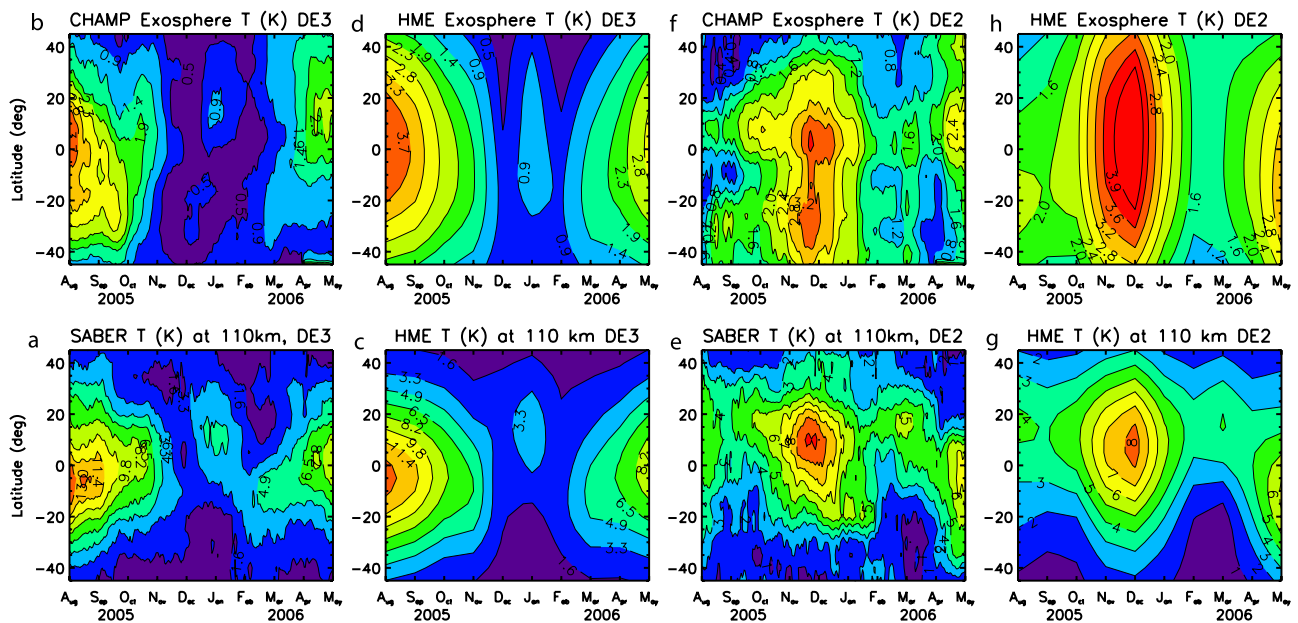


Figure 3. Latitude structures of *DE3* and *DE2* non-migrating diurnal tidal temperature amplitudes and comparisons with Hough Mode Extension (HME) approximations during August 2005–May 2006. (a) SABER *DE3* temperature amplitudes at 110 km (max 13K), (b) *DE3* exosphere temperature amplitudes (max 3.3K), (c) *DE3* temperature amplitudes from HME fit to SABER temperatures (max 13K), and (d) *DE3* exosphere temperature amplitudes predicted by *DE3* upward extension (max 3.7K). Same as Figures 3a–3d, except for *DE2*, with respective maxima of (e) 9K, (f) 3.2K, (g) 8K, and (h) 3.9K.

surface. Similar effects are likely to occur on Mars where topographic forcing of non-migrating tides is intense [Moudden and Forbes, 2008], and recent observational evidence suggests that this indeed may be the case [Mazarico *et al.*, 2008]. It does raise the question, though, as to whether potential exosphere variability at Mars due to non-migrating tides may have influenced atmospheric escape, now or in the past.

[14] **Acknowledgments.** J. Forbes was supported by grant ATM-0719480 from the National Science Foundation as part of the Space Weather Program and AFOSR MURI award FA9550-07-1-0565. J. Oberheide was supported by grant OB 299-2/2 from the Deutsche Forschungsgesellschaft as part of its CAWSES priority program. The accelerometer and flight data for this project were made available by the Geoforschungszentrum (GFZ), Potsdam, Germany.

References

- Angelats i Coll, M., and J. M. Forbes (2002), Nonlinear interactions in the upper atmosphere: The $s = 1$ and $s = 3$ nonmigrating semidiurnal tides, *J. Geophys. Res.*, *107*(A8), 1157, doi:10.1029/2001JA900179.
- Bruinsma, S., D. Tamagnan, and R. Biancale (2004), Atmospheric densities derived from CHAMP/STAR accelerometer observations, *Planet. Space Sci.*, *52*, 297–312.
- Bruinsma, S., J. M. Forbes, R. S. Nerem, and X. Zhang (2006), Thermosphere density response to the 20–21 November 2003 solar and geomagnetic storm from CHAMP and GRACE accelerometer data, *J. Geophys. Res.*, *111*, A06303, doi:10.1029/2005JA011284.
- Conrath, B. J. (1976), Influence of planetary-scale topography on the diurnal thermal tide during the 1971 Martian dust storm, *J. Atmos. Sci.*, *33*, 2430–2439.
- Forbes, J. M., and H. B. Garrett (1979), Theoretical studies of atmospheric tides, *Rev. Geophys. Space Phys.*, *17*, 1951–1981.
- Forbes, J. M., and M. E. Hagan (2000), Diurnal Kelvin wave in the atmosphere of Mars: Towards an understanding of “stationary” density structures observed by the MGS accelerometer, *Geophys. Res. Lett.*, *27*, 3563–3566.
- Forbes, J. M., A. F. C. Bridger, S. W. Bougher, M. E. Hagan, J. L. Hollingsworth, G. M. Keating, and J. Murphy (2002), Nonmigrating tides in the thermosphere of Mars, *J. Geophys. Res.*, *107*(E11), 5113, doi:10.1029/2001JE001582.
- Forbes, J. M., J. Russell, S. Miyahara, X. Zhang, S. Palo, M. Mlynczak, C. J. Mertens, and M. E. Hagan (2006), Troposphere-thermosphere tidal coupling as measured by the SABER instrument on TIMED during July–September 2002, *J. Geophys. Res.*, *111*, A10S06, doi:10.1029/2005JA011492.
- Forbes, J. M., X. Zhang, S. Palo, J. Russell, M. Mlynczak, and C. J. Mertens (2008), Tidal variability in the ionospheric dynamo region, *J. Geophys. Res.*, *113*, A02310, doi:10.1029/2007JA012737.
- Hagan, M. E., and J. M. Forbes (2002), Migrating and nonmigrating diurnal tides in the middle and upper atmosphere excited by tropospheric latent heat release, *J. Geophys. Res.*, *107*(D24), 4754, doi:10.1029/2001JD001236.
- Hagan, M. E., and J. M. Forbes (2003), Migrating and nonmigrating semidiurnal tides in the middle and upper atmosphere excited by tropospheric latent heat release, *J. Geophys. Res.*, *108*(A2), 1062, doi:10.1029/2002JA009466.
- Hagan, M. E., A. Maute, and R. G. Roble (2009), Tropospheric tidal effects on the middle and upper atmosphere, *J. Geophys. Res.*, *114*, A01302, doi:10.1029/2008JA013637.
- Lühr, H., K. Häusler, and C. Stolle (2007), Longitudinal variation of F region electron density and thermospheric zonal wind caused by atmospheric tides, *Geophys. Res. Lett.*, *34*, L16102, doi:10.1029/2007GL030639.
- Mazarico, E., M. T. Zuber, F. G. Lemoine, and D. E. Smith (2008), Observation of atmospheric tides in the Martian exosphere using Mars Reconnaissance Orbiter radio tracking data, *Geophys. Res. Lett.*, *35*, L09202, doi:10.1029/2008GL033388.
- Moudden, Y., and J. M. Forbes (2008), Topographic connections with density waves in Mars’ aerobraking regime, *J. Geophys. Res.*, *113*, E11009, doi:10.1029/2008JE003107.
- Oberheide, J., and J. M. Forbes (2008), Tidal propagation of deep tropical cloud signatures into the thermosphere from TIMED observations, *Geophys. Res. Lett.*, *35*, L04816, doi:10.1029/2007GL032397.
- Picone, J. M., A. E. Hedin, D. P. Drob, and A. C. Aikin (2002), NRLMSISE-00 empirical model of the atmosphere: Statistical comparisons and scientific issues, *J. Geophys. Res.*, *107*(A12), 1468, doi:10.1029/2002JA009430.

- Svoboda, A. A., J. M. Forbes, and S. Miyahara (2005), A space-based climatology of MLT winds, temperatures and densities from UARS wind measurements, *J. Atmos. Sol. Terr. Phys.*, *67*, 1533–1543.
- Yagai, I. (1989), Nonmigrating thermal tides detected in data analysis and a general circulation model simulation, *J. Geophys. Res.*, *94*, 6341–6356.
- Zhang, X., J. M. Forbes, J. Russell, S. Palo, M. Mlynczak, C. J. Mertens, and M. E. Hagan (2006), Monthly tidal temperatures 20–120 km from TIMED/SABER, *J. Geophys. Res.*, *111*, A10S08, doi:10.1029/2005JA011504.
- Zurek, R. W. (1976), Diurnal tide in the Martian atmosphere, *J. Atmos. Sci.*, *33*, 321–337.
-
- S. L. Bruinsma, Department of Terrestrial and Planetary Geodesy, Centre Nationale D'Etudes Spatiales, F-31401 Toulouse, France. (sean.bruinsma@cnes.fr)
- J. M. Forbes and X. Zhang, Department of Aerospace Engineering Sciences, University of Colorado, Boulder, CO 80309, USA. (forbes@colorado.edu; xiaoli.zhang@colorado.edu)
- J. Oberheide, Physics Department, University of Wuppertal, D-42119 Wuppertal, Germany. (joberh@uni-wuppertal.de)